Korean J. Chem. Eng., **20**(2), 328-333 (2003)

Modeling of Absorption of NO_2 with Chemical Reaction in a Falling Raindrop

Vishnu Pareek†, Vinod K. Srivastava* and Adesoji A. Adesina**

Department of Chemical Engineering, Curtin University of Technology, GPO Box U1987, Perth, WA, 6845, Australia
*Department of Chemical Engineering, Indian Institute of Technology Hauz Khas, New Delhi, India
**School of Chemical Engineering and Industrial Chemistry, University of New South Wales, Sydney 2052, Australia
(*Received 28 August 2001 • accepted 29 August 2002*)

Abstract−A model has been proposed for the scavenging of NO_2 in a falling raindrop. After absorption, aqueous NO_2 undergoes a second order reaction to form various ions such as NO_2^-, NO_3^- and H^+. The model is based on the unsteady state convective diffusion equation, which was solved for given boundary conditions by using implicit alternate direction (ADI) method. The circulation of fluid inside and outside the raindrop has been taken into account to realistically describe the flow field in the numerical domain. The model predictions indicate that the pH of a raindrop is a direct function of the drop size and bulk concentration of NO_2. The model predicted a pH of about 4.9 for a 100-micron raindrop falling through a 20-ppb ambient concentration of NO_2. For the same ambient concentration of NO_2, a 10-micron raindrop would have a pH of about 4.75. The predictions also suggested that for all practical purposes the gas phase resistance may be taken as the rate-controlling step. The predicted values of gas-side mass transfer coefficient compared well with the estimated values using standard mass transfer correlations.

Key words: Absorption, Acid Rain, Scavenging, Raindrop, Finite Difference

INTRODUCTION

Large quantities of polluting gases (such as SO_x and NO_x) are introduced into the atmosphere through a variety of industrial and automobile activities. These gases can directly affect the welfare of the ecosystem around the intense source through dry deposition. However, the widespread effect on the ecosystem is caused by the absorption of these gases in rainwater, which can decrease the pH of rainwater appreciably, thus leading to a phenomenon called acid rain. As rainwater is in equilibrium with the atmospheric carbon dioxide, which yields a natural acidity with a pH of about 5.6 [Seinfeld, 1986], a pH of less than 5.6 may be considered an indication of SO_2 and NO_x absorption.

A number of attempts have been made to describe the mechanism of trace gas scavenging in a falling raindrop for SO_2 absorption and its subsequent transformation to various chemical species [Hales, 1972; Baboolal et al., 1981]. However, the data on the absorption of NO_x in a raindrop are scarce, even though in many areas of the world they have been found to contribute significantly to the acidity in the rainwater [Ahmed et al., 1990]. Furthermore, a majority of the reported studies on NO_x in the literature focussed on the measurement of chemical composition of rainwater [Saxena et al., 1996]. Relatively few laboratory studies have been carried out to establish the pathways by which the oxides of nitrogen are converted to various species after they are absorbed in water [Bambauer et al., 1994; Schwartz and White, 1981, 1983]. Although useful qualitative information can be obtained from such measurements, especially with regards to the deposition rate, no quantitative information is available on the efficiency with which a particular gas in the atmosphere is scavenged by rain.

†To whom correspondence should be addressed.
E-mail: v.pareek@curtin.edu.au

To overcome this difficulty a number of acid rain models have been reported [Metcalfe et al., 2001]. Most of these models are statistical in nature and are used by various environmental agencies in the formulation of acid rain control policies. The Hull Acid Rain Model (HARM) [Metcalfe et al., 2001], extensively used by the UK government for the control of acidification of rain, is a receptor oriented Lagrangian statistical model. These models, however, do not estimate the efficiencies with which drop of a given size scavenges NO_2. In this paper we present a model for scavenging of NO_2 in a falling raindrop. The model is based on the unsteady state convective diffusion equation, which was solved by using a finite difference approximation scheme called implicit alternate direction (ADI) method [Carnahan et al., 1969]. The only model inputs are raindrop size and prevailing NO_2 concentration. A falling raindrop exhibits vigorous internal circulation. Therefore, to realistically describe the flow-field inside and outside the raindrop, the velocity relations reported by LeClair et al. [1972] were incorporated in the model. The model is capable of predicting pH levels likely to be achieved by a raindrop falling through a given ambient NO_2 concentration; hence, it can be used to set the ambient limits on the emission of NO_2 for the allowed levels of rain pH.

THEORETICAL CONSIDERATIONS

1. Model Equations and Boundary Conditions

For diffusion of NO_2 inside a falling raindrop, the general convective diffusion equation [Bird et al., 1960] (on neglecting azimuthal coordinate) reduces to:

$$\frac{\partial C_{A,in}}{\partial t} = D_{AL}\left(\frac{\partial^2 C_{A,in}}{\partial r^2} + \frac{\cot\theta}{r^2}\frac{\partial C_{A,in}}{\partial \theta} + \frac{1}{r^2}\frac{\partial^2 C_{A,in}}{\partial \theta^2} + \frac{2}{r}\frac{\partial C_{A,in}}{\partial r}\right) - v_r\frac{\partial C_{A,in}}{\partial r} - \frac{v_\theta}{r}\frac{\partial C_{A,in}}{\partial \theta} - k_2 C_{A,in}^2 \quad (1)$$

and for outside the raindrop we have:

$$\frac{\partial C_{A,out}}{\partial t}=D_{AG}\left(\frac{\partial^2 C_{A,out}}{\partial r^2}+\frac{\cot\theta\partial C_{A,out}}{r^2\partial\theta}+\frac{1}{r^2}\frac{\partial^2 C_{A,out}}{\partial\theta^2}+\frac{2}{r}\frac{\partial C_{A,out}}{\partial r}\right)$$
$$-v_r\frac{\partial C_{A,out}}{\partial r}-\frac{v_\theta}{r}\frac{\partial C_{A,out}}{\partial\theta} \quad (2)$$

where, $C_{A,in}$ and $C_{A,out}$ denote the concentration of NO_2 inside and outside of the raindrop, v_r and v_θ are components of velocity in the radial and angular directions, respectively. Eqs. (1) and (2) were solved by using following boundary and initial conditions:

(1) At t=0, $C_{A,in}=0$ (for all $a\geq r\geq 0$ and $\pi\geq\theta\geq 0$)
(2) At $\theta=0$ and π, $(\partial C_{A,in}/\partial\theta)=0$ (for all $a\geq r\geq 0$ and $t>0$)
(3) At r=0, $(\partial C_{A,in}/\partial r)=0$ (for all $t>0$ and $\pi\geq\theta\geq 0$)
(4) At r=a, $D_{AL}\frac{\partial C_{A,in}}{\partial r}=D_{AG}\frac{\partial C_{A,out}}{\partial r}$ (for all $t>0$ and $\pi\geq\theta\geq 0$)
(5) At t=0, $C_{A,out}=C_{Ao,out}$ (for all $r>a$ and $\pi\geq\theta\geq 0$)
(6) At $\theta=0$ and π, $(\partial C_{A,out}/\partial\theta)=0$ (for all $r>a$ and $t>0$)
(7) At $r=\infty$ $C_{A,out}=C_{Ao,out}$ (for all $t>0$)

Introducing dimensionless variables

$$T=\frac{D_{AL}t}{a^2},\ N_{Peclet,L}=\frac{2aV_o}{D_{AL}},\ N_{Peclet,G}=\frac{2aV_o}{D_{AG}},$$
$$C_{in}=\frac{C_{A,in}}{C_{Ao,in}},\ C_{out}=\frac{C_{A,out}}{C_{Ao,out}},\ H_A=\frac{C_{Ao,out}}{C_{Ao,in}},$$
$$V_R=\frac{v_r}{V_o},\ V_\theta=\frac{v_\theta}{V_o},\ D=\frac{D_{AL}}{D_{AG}},\ R=\frac{r}{a}\text{ and }k=\frac{k_2C_{Ao,in}a^2}{D_{AL}}$$

the Eqs. (1) and (2) become:

$$\frac{\partial C_{in}}{\partial T}=\left(\frac{\partial^2 C_{in}}{\partial R^2}+\frac{\cot\theta\partial C_{in}}{R^2\partial\theta}+\frac{1}{R^2}\frac{\partial^2 C_{in}}{\partial\theta^2}+\frac{2}{R}\frac{\partial C_{in}}{\partial r}\right)$$
$$-\frac{N_{Peclet,L}}{2}\left(V_R\frac{\partial C_{in}}{\partial R}+\frac{V_\theta}{R}\frac{\partial C_{in}}{\partial\theta}\right)-kC_{in}^2 \quad (1A)$$

$$D\frac{\partial C_{out}}{\partial T}=\left(\frac{\partial^2 C_{out}}{\partial R^2}+\frac{\cot\theta\partial C_{out}}{R^2\partial\theta}+\frac{1}{R^2}\frac{\partial^2 C_{out}}{\partial\theta^2}+\frac{2}{R}\frac{\partial C_{out}}{\partial R}\right)$$
$$-\frac{N_{Peclet,G}}{2}\left(V_R\frac{\partial C_{out}}{\partial R}+\frac{V_\theta}{R}\frac{\partial C_{out}}{\partial\theta}\right) \quad (2A)$$

with the new initial and boundary conditions:

(1A) At T=0, $C_{in}=0$ (for all $1\geq R\geq 0$ and $\pi\geq\theta\geq 0$)
(2A) At $\theta=0$ and π, $(\partial C_{in}/\partial\theta)=0$ (for all $1\geq R\geq 0$ and $T>0$)
(3A) At r=0, $(\partial C_{in}/\partial R)=0$ (for all $T>0$ and $\pi\geq\theta\geq 0$)
(4A) At r=a, $D\frac{\partial C_{in}}{\partial R}=H_A\frac{\partial C_{out}}{\partial R}$ (for all $T>0$ and $\pi\geq\theta\geq 0$)
(5A) At t=0, $C_{out}=1$ (for all $R>1$ and $\pi\geq\theta\geq 0$)
(6A) At $\theta=0$ and π, $(\partial C_{out}/\partial\theta)=0$ (for all $R>1$ and $T>0$)
(7A) At $R=\infty$ $C_{out}=1$ (for all $T>0$)

As pointed out earlier a falling raindrop exhibits vigorous internal circulation as shown in Fig. 1. The flow-field outside the raindrop is also affected by drag force of atmospheric air. The dimensionless components of velocity profiles both inside and outside the raindrop are given by [LeClair et al., 1972]:

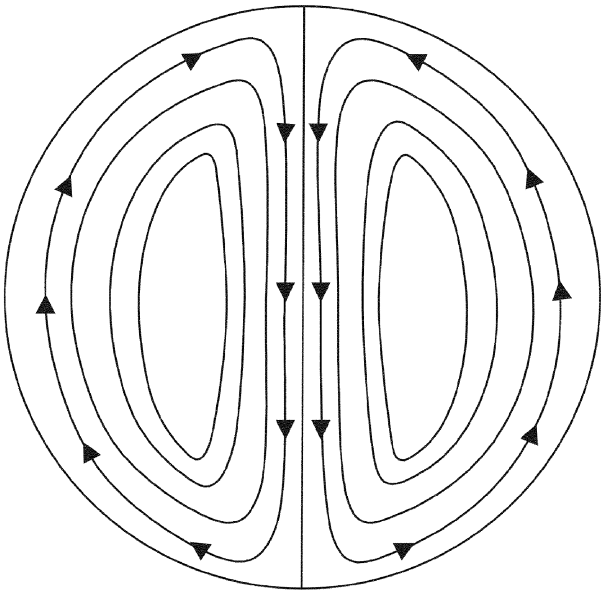

Fig. 1. Flow field inside a falling raindrop.

Inside the raindrop:

$$V_R=-\frac{\sigma}{2(1+\sigma)}(R^2-1)\cos\theta \quad (3)$$

$$V_\theta=-\frac{\sigma}{2(1+\sigma)}(2R^2-1)\sin\theta \quad (4)$$

Outside the raindrop:

$$V_R=\left(\frac{3+2\sigma}{2(1+\sigma)}R-\frac{1}{2(1+\sigma)}R^3-1\right)\cos\theta \quad (5)$$

$$V_\theta=\left(\frac{3+2\sigma}{4(1+\sigma)}R-\frac{1}{4(1+\sigma)}R^3+1\right)\sin\theta \quad (6)$$

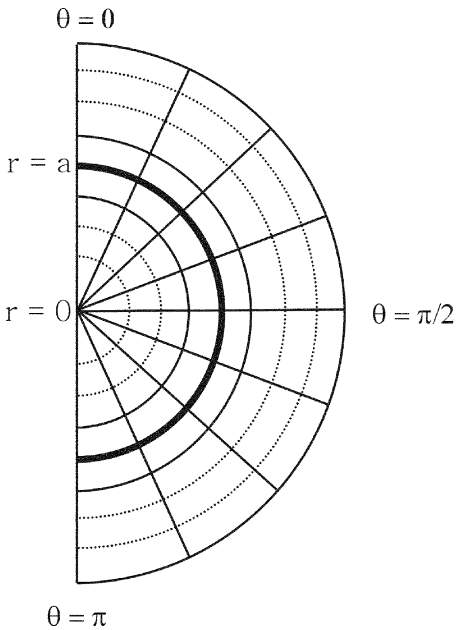

Fig. 2. A typical numerical grid.

where, σ is the viscosity ratio (water to air).

The terminal velocities V_o of falling raindrops were estimated by using the method outlined by Beard [1976].

2. Solution Scheme

The partial differential Eqs. (1) and (2) were solved by using a finite difference approximation scheme called the implicit alternate direction (ADI) method [Carnahan et al., 1969]. A sample of numerical grids utilized in the calculations is shown in Fig. 2. The scheme consists of two steps:

(1) Explicit scheme for θ-direction and implicit scheme for r-direction in the first half of the step-time.

(2) Explicit scheme for r-direction and implicit scheme for θ-direction in the next half of the step-time.

As this scheme is a hybrid of explicit and implicit schemes, it enjoys the advantages of both and was found to be very stable, with the convergence typically achieved within 50 iterations. Discretization of the space inside and outside the raindrop was achieved by using an ingeniously developed Fortran code called ADIAN (see Appendix A). The application of the scheme to Eqs. (1) and (2) gave a set of linear equations, with a tridiagonal coefficient matrix, which were readily solved using a subroutine called MATRIX [Srivastava, 1981].

3. Physical and Chemical Data

The diffusivities of NO_2 in air and water were calculated by using the Fuller method and Wilke-Chang equation, respectively [Bird et al., 1960]. The estimated value of D_{AL} at ambient temperature (20 °C) was 2.74×10^{-9} m^2 s^{-1} and that of D_{AG} was 1.77×10^{-5} m^2 s^{-1}. The value of Henry's equilibrium constant H_A for the absorption of NO_2 in water was taken as 1.0×10^{-2} mol L^{-1} atm^{-1} [Scheartz and White, 1983]. The aqueous oxidation of NO_2 has a second order kinetics [Seinfeld, 1986] with the rate constant $k_2=4.25\times10^7$ mol^{-1} L s^{-1}.

RESULTS AND DISCUSSION

The performance of the model described above was evaluated with respect to variation in drop size and ambient concentration of NO_2. Fig. 3 shows radial concentration profiles inside and outside a 100-micron raindrop falling through an ambient NO_2 concentration of 80 ppm after a falling-time of 0.5 sec. Inside the raindrop (referred as bulk liquid in Fig. 3), the concentration profiles for various angular coordinates showed a maximum at a dimensionless radial distance of about 0.65. This effect may be attributed to the internal circulation within the raindrop. It is apparent from Fig. 3 that in the beginning of its fall (t<0.5 s) NO_2 concentration decreased with increased angular coordinate. This is because in the lower hemisphere ($\theta\geq\pi/2$), the fluid flows in the opposite direction (Fig. 1) to diffusion, while in the upper hemisphere ($\theta\leq\pi/2$) both momentum and diffusional transport are in the same direction, thus enhancing mass transfer. As may be expected, this effect was less pronounced in the smaller raindrops. (cf. Fig. 4).

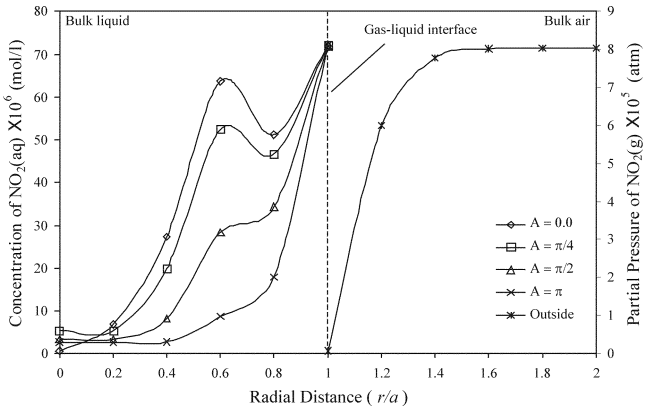

Fig. 3. Radial concentration profiles of NO_2 (aq) after a time of 0.5 s (Drop size=100 micron, ambient NO_2 concentration =80 ppm).

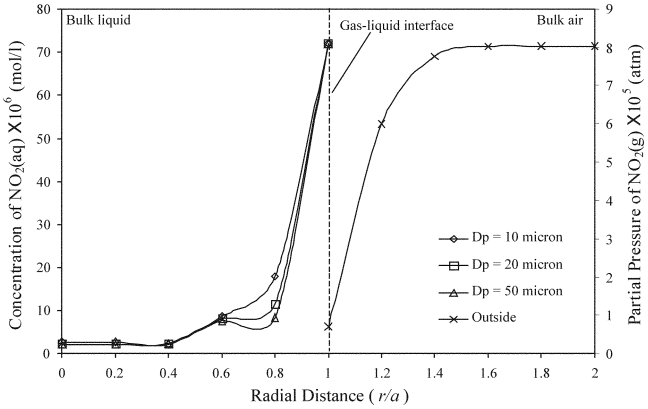

Fig. 4. Radial concentration profiles of NO_2 (aq) after a time of 0.5 s for different drop sizes (Angular coordinate=0, ambient NO_2 concentration =80 ppm).

Furthermore, the model predictions indicated that NO_2 concentration was essentially invariant with angular coordinate outside the raindrop. Fig. 3 also shows that the gas phase NO_2 concentration dropped rather sharply from 80 ppm in the bulk to about 0.7 ppm at the gas-liquid interface suggesting that gas film resistance was probably the rate-controlling step. For mass transfer into a spherical drop, Frossing's correlation [Bird et al., 1960] gives, $k_g=0.215$ m s^{-1} ($K_g=3.96\times10^{-3}$ mol m^{-3} s^{-1} atm^{-1}). Assuming that the film theory describes the mechanism for NO_2 transport from the gas into the raindrop, the data from Fig. 3 may be used to estimate $k_g=D_{AG}/z$ as 0.169 m s^{-1} ($K_g=3.10\times10^{-3}$ mol m^{-3} s^{-1} atm^{-1}). The good comparison between predicted data and literature correlation further strengthened the confidence in the unsteady state convective diffusion model proposed in this work. Moreover, applying the criterion

$$\frac{K_g P_{Ao}}{k_2 C_{Ao,in}^2} \ll 1$$

for the gas-film controlling step, the present data provide the LHS as 9.1×10^{-3} and hence it may be confirmed that gas-side resistance was the controlling step.

Angular concentration profiles associated with the radial profiles in Fig. 3 are shown in Fig. 5. A snapshot of the angular concentration profiles shows that the aqueous NO_2 concentration decreased with angular coordinate (θ) irrespective of the radial distance selected. However, apparent intersection of some of the profiles was

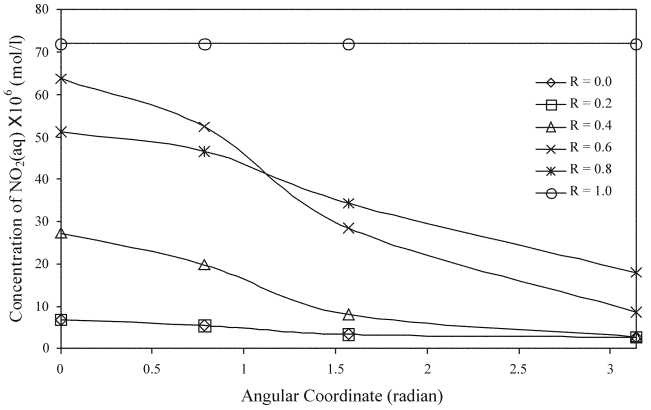

Fig. 5. Angular concentration profiles of NO_2 (aq) after a time of 0.5 s (Drop size=100 micron, ambient NO_2 concentration =80 ppm).

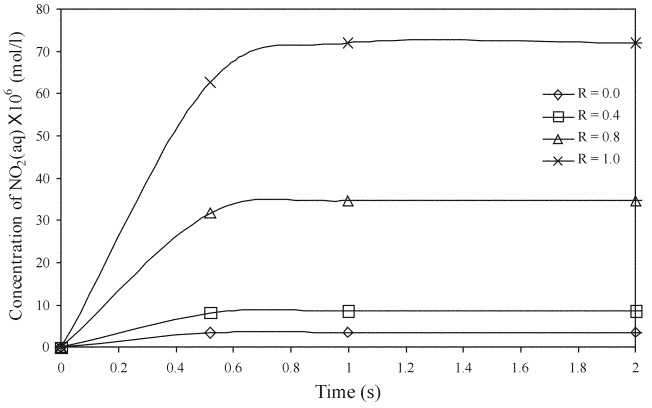

Fig. 6. Variation in concentration of NO_2 (aq) at different radial coordinates (Drop size=100 micron, ambient NO_2 concentration =80 ppm).

due to a combination of unsteady state conditions and internal recirculation of the liquid within the raindrop. As may be seen in Fig. 6, steady state was obtained after about 1 sec.

As a result of NO_2 absorption, the concentration of H^+-ions inside the raindrop increased. A concentration history of H^+-ions is shown in Fig. 7. As may be readily seen in the Figure, the smaller drops had a higher concentration of H^+-ions at a given time. For example a 10-micron drop achieved an H^+-ion concentration of about 2×10^{-5} mol L^{-1} after a falling time of 1 s, for the similar duration the H^+-ions concentration for a 200-micron drop was only about 8×10^{-6} mol L^{-1}. Furthermore, the smaller drops achieved an equilibrium concentration of H^+-ions earlier than the larger drop.

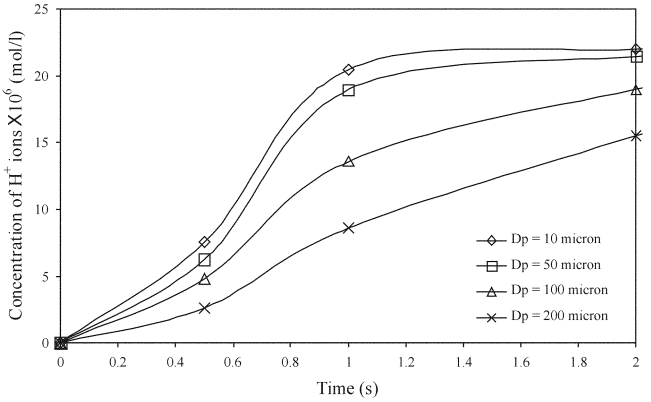

Fig. 7. Variation in concentration of H^+ ions (Ambient NO_2 concentration=100 ppb).

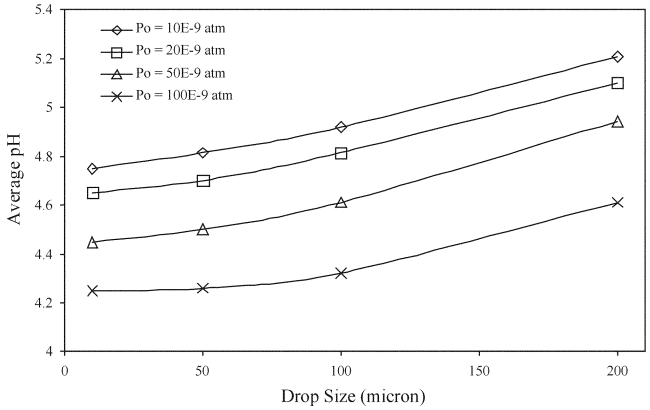

Fig. 8. Average final pH Vs drop size.

The increase in H^+-ions concentration led to a decrease in the water pH. Fig. 8 shows the effect of raindrop size and bulk concentration of NO_2 on the final average pH (allowing a drop time of 5 s) achieved by a falling raindrop. The pH dropped exponentially with the increase in ambient NO_2 partial pressure and with decrease in raindrop size. It is therefore clear that the pH of raindrop is very sensitive to the increase in NO_2 concentration and drop size. For example, a raindrop of average size of 100-micron can achieve a pH as low as 4.4 when falling through an NO_2 concentration of about 100 ppb.

The effect of liquid side Peclet number $N_{Peclet,L}=2aV_o/D_{AL}$ on NO_2 concentration is shown in Fig. 9. By definition, Peclet number in this case is a direct measure of drop size and its terminal velocity; therefore, it may be taken as a direct measure of the circulation effects within the raindrop. As indicated above, the angular gradient in concentration of NO_2 was mainly due to the circulation effects.

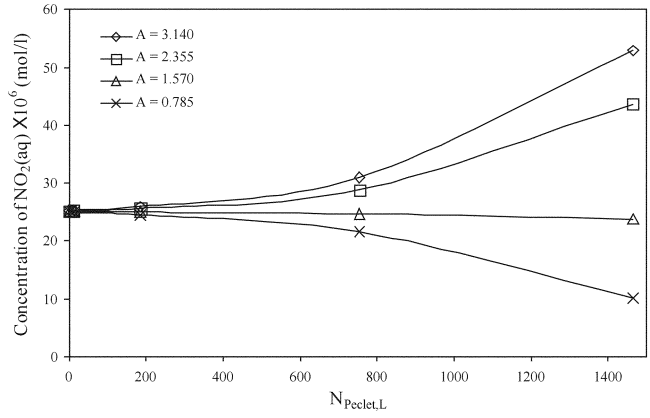

Fig. 9. Effect of Peclet number on concentration of NO_2 (aq) after a time of 0.5 s (Drop size=100 micron, ambient NO_2 concentration=80 ppm).

At lower values of Peclet number, when the circulation effects were negligible, various constant A curves coincided with each other as shown in Fig. 9. For higher values of Peclet number the concentration profiles corresponding to different values of angular vector A diverged away from each other, indicating the dominance of circulation effects. Interestingly, the concentration profile for $A=\pi/2$ was almost independent of the Peclet number. This was apparently due to the fact that at $A=\pi/2$, all the velocity-vectors within the rain drop were parallel to each other and were pointing vertically upwards or downwards and there was no component of velocity pointing in the direction of diffusion. Hence, the concentration profile at $A=\pi/2$, was free of the circulation effects.

CONCLUDING REMARK

An acid rain model for the scavenging of NO_2 has been developed. The model is based on the unsteady state convective diffusion equation. The underlying partial differential equations were solved by using the implicit alternate direction method to avoid numerical instabilities. The internal circulation effects played an important role in the beginning of the absorption of NO_2 in the falling raindrop. The predicted results showed that the pH of a falling raindrop was very sensitive towards variation in bulk concentration of NO_2 and drop size. Since the model is based on the unsteady state absorption of species, it adequately describes the mechanism of trace gas scavenging.

APPENDIX A

The alternate direction implicit (ADI) method utilizes the advantage of both implicit and explicit finite difference schemes. In general, it is stable, convergent and is not computer memory intensive [Carnahan and Wilkes, 1969]. In this study, the ADI method constituted the fol1owing two steps:

1. Explicit Scheme for θ-Direction and Implicit Scheme for r-Direction for the First Half of the Time-step

1-1. For Inside the Drop

On employing the scheme to Eq. (1A), we have,

$$AC_{in,ij}^{n+1/2}+B_{ij}C_{in,i+1,j}^{n+1/2}+D_{ij}C_{in,i-1,j}^{n+1/2}=E_{ij}^{n}. \quad (A1)$$

where,

$$A=\frac{1}{\Delta T}+\frac{2}{(\Delta R)^2}$$

$$B_{ij}=F_{ij}-\frac{1}{(\Delta R)^2}$$

$$D_{ij}=-F_{ij}-\frac{1}{(\Delta R)^2}$$

$$E_{ij}^{n}=G_iC_{in,ij}^{n}+H_{ij}C_{in,i,j-1}^{n}+I_{ij}C_{in,i,j+1}^{n}-k(C_{in,ij}^{n})^2$$

$$F_{ij}=-\frac{1}{R_i(\Delta R)}+\frac{N_{Pe}V_{R,ij}}{4\Delta R}$$

$$G_i=\frac{1}{\Delta T}-\frac{2}{R_i^2(\Delta\theta)^2}$$

$$H_{ij}=J_{ij}+\frac{1}{R_i^2(\Delta\theta)^2}$$

$$I_{ij}=-J_{ij}+\frac{1}{R_i^2(\Delta\theta)^2}$$

$$J_{ij}=\frac{\cot(\theta_j)}{2R_i^2(\Delta\theta)}+\frac{N_{Pe}V_{\theta,ij}}{4R_i\Delta\theta}$$

The superscript n represents the time-step, subscripts i and j represent radial and angular discretizations respectively. Superscript (n+1/2) in LHS of Eq. (A1) represents the value at half time-step.

1-2. For Outside the Raindrop

Similarly, the application of the ADI method outside the raindrop (Eq. 2A) yielded,

$$AC_{out,ij}^{n+1/2}+B_{ij}C_{out,i+1,j}^{n+1/2}+D_{ij}C_{out,i-1,j}^{n+1/2}=L_{ij}^{n}. \quad (A2)$$

where,

$$L_{ij}^{n}=G_iC_{out,ij}^{n}+H_{ij}C_{out,i,j-1}^{n}+I_{ij}C_{out,i,j+1}^{n}$$

2. Implicit Scheme for θ-Direction and Explicit Scheme for r-Direction for the Second Half of the Time-step

2-1. Inside the Raindrop

On using the implicit scheme for θ-direction and explicit scheme for r-direction for the next half of the time-step, we have,

$$M_iC_{in,ij}^{n+1}+N_{ij}C_{in,i,j+1}^{n+1}+O_{ij}C_{in,i,j-1}^{n+1}=P_{ij}^{n+1/2}. \quad (A3)$$

where,

$$M_i=\frac{1}{\Delta T}+\frac{2}{R_i^2(\Delta\theta)^2}$$

$$N_{ij}=J_{ij}-\frac{1}{R_i^2(\Delta\theta)^2}$$

$$O_{ij}=-J_{ij}-\frac{1}{R_i^2(\Delta\theta)^2}$$

$$P_{ij}^{n+1/2}=QC_{in,ij}^{n+1/2}+S_{ij}C_{in,i+1,j}^{n+1/2}+U_{ij}C_{in,i-1,j}^{n+1/2}-k(C_{ij}^{n+1/2})^2$$

$$Q=\frac{1}{\Delta T}-\frac{2}{(\Delta\theta)^2}$$

$$S_{ij}=-F_{ij}+\frac{1}{(\Delta R)^2}$$

$$U_{ij}=F_{ij}+\frac{1}{(\Delta R)^2}$$

2-2. For Outside the Raindrop

Similarly, for outside the raindrop,

$$M_iC_{out,ij}^{n+1}+N_{ij}C_{out,i,j+1}^{n+1}+O_{ij}C_{out,i,j-1}^{n+1}=W_{ij}^{n+1/2}. \quad (A4)$$

where,

$$W_{ij}^{n+1/2}=QC_{out.ij}^{n+1/2}+S_{ij}C_{out.i+1,j}^{n+1/2}+U_{ij}C_{out.i-1,j}^{n+1/2}$$

On using boundary conditions (1A-7A), Eqs. (A1-A4) reduced to a set of tri-diagonal matrices, which were then solved by using MATRIX [Srivastava, 1981]. The flux condition at the surface of the raindrop was incorporated by an iterative method.

NOMENCLATURE

a : radius of raindrop [m]
A : angular coordinate [radian]
$C_{A,in}$: concentration of NO_2 inside the drop [mol L^{-1}]
$C_{A,out}$: concentration of NO_2 outside the drop [mol L^{-1}]
$C_{Ao,in}$: initial concentration of NO_2 inside the drop [mol L^{-1}]
$C_{Ao,out}$: initial concentration of NO_2 outside the drop [mol L^{-1}]
C_{in} : $C_{A,in}/C_{Ao,in}$

C_{out} : $C_{A,\,out}/C_{Ao,\,out}$
D : D_{AL}/D_{AG}
D_{AL} : diffusivity of NO_2 in water [$m^2\ s^{-1}$]
D_{AG} : diffusivity of NO_2 in air [$m^2\ s^{-1}$]
D_p : rain drop diameter [m]
H_A : Henry's constant for absorption of NO_2 in water [mol L^{-1} atm^{-1}]
k : dimensionless rate constant, $k = \frac{k_2 C_{Ao,in} a^2}{D_{AL}}$
k_2 : rate constant [$mol^{-1}\ L\ s^{-1}$]
k_g : gas side mass transfer coefficient [m s^{-1}]
K_g : gas side mass transfer coefficient based on partial pressure [mol m^{-3} s^{-1} atm^{-1}]
$N_{Peclet,\,L}$: liquid side Peclet number ($2aV_o/D_{AL}$)
$N_{Peclet,\,G}$: gas side Peclet number ($2aV_o/D_{AG}$)
P_{O2} : partial pressure of oxygen [atm]
r : radial vector measured from the center of raindrop [m]
R : dimensionless radial coordinate (r/a)
t : time [s]
T : dimensionless time ($D_{AL}t/a^2$)
v_r : radial component of velocity [m s^{-1}]
v_θ : angular component of velocity [m s^{-1}]
V_o : terminal velocity of raindrop [m s^{-1}]
V_R : dimensionless radial component of velocity, (v_r/V_o)
V_θ : dimensionless angular component of velocity, (v_θ/V_o)
z : mass transfer film thickness [m]

Greek Letters

θ : angular vector
σ : ratio of viscosity of water to viscosity of air

REFERENCES

Ahmed, A. F. M., Singh, R. P. and Elmubarak, A. H., "Chemistry of Atmospheric Precipitation at the Western Arabian Gulf," *Atmospheric Environment*, **24A**, 2927 (1990).

Baboolal, L. B., Pruppacher, H. R. and Topalian, J. H., "A Sensitivity Study of a Theoretical Model of SO_2 Scavenging by Water Drops in Air," *Journal of the Atmospheric Sciences*, **38**, 856 (1981).

Bambauer, A., Brantner, B., Paige, M. and Novakov, T., "Laboratory Study of NO_2 Reaction with Dispersed and Bulk Liquid Water," *Atmospheric Environment*, **28**, 3225 (1994).

Beard, K. V., "Terminal Velocity and Shape of Cloud and Rain Drops Aloft," *Journal of the Atmospheric Sciences*, **33**, 851 (1976).

Bird, R. B., Stewart, W. E. and Lightfoot, E. N., "Transport Phenomena," John Wiley & Sons, New York (1960).

Carnahan, B., Luther, H. A. and Wilkes, J. O., "Applied Numerical Methods," John Wiley and Sons, New York (1969).

Hales, J. M., "Fundamentals of the Theory of Gas Scavenging by Rain," *Atmospheric Environment*, **6**, 635 (1972).

LeClair, B. P., Hamielec, A. E., Pruppacher, H. R. and Hall, W. D., "A Theoretical and Experimental Study of the Internal Circulation in Water Drops Falling at Terminal Velocity in Air," *Journal of the Atmospheric Sciences*, **29**, 728 (1972).

Metcalfe, S. E., Whyatt, J. D., Broughton, R., Derwent, R. G., Finnegan, D., Hall, J., Mineter, M., O'Donoghue, M. and Shutton, M. A., "Developing A Hull Acid Rain Model: Its Validation and Implications for Policy Makers," *Environmental Science and Policy*, **4**, 25 (2001).

Saxena, A., Kulshrestha, U. C., Kumar, N., Kumari, K. M. and Srivastava, S. S., "Characterization of Precipitation at Agr," *Atmospheric Environment*, **30**, 3405 (1996).

Schwartz, S. E. and White, W. H., "Kinetics of Reactive Dissolution of Nitrogen Oxides into Aqueous Solution," *Advanced Environmental Science and Technology*, **12**, 1 (1983).

Schwartz, S. E. and White, W. H., "Solubility Equilibria of the Nitrogen Oxides and Oxy-Acids in Dilute Aqueous Solution," *Advanced Environmental Science and Technology*, **4**, 1 (1981).

Seinfeld, J. H., "Atmospheric Chemistry and Physics of Air Pollution," John Wiley and Sons, New York, 195 (1986).

Srivastava, V. K., "The Thermal Cracking of Benzene in a Pipe Reactor," Ph.D. Thesis, University of Wales, Swansea (UK) (1981).